AFRL-VS-TR-1999-1537

MESOSCALE IONOSPHERIC PHENOMENA

Tom Chang

Massachusetts Institute of Technology
Center for Space Research
Center for Theoretical Geo/Cosmo Plasma Physics
Cambridge, MA 02139

1 Nov 1999

Final Report

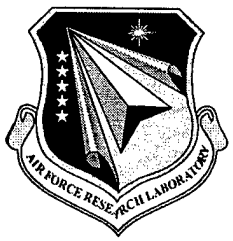

AIR FORCE RESEARCH LABORATORY
Space Vehicles Directorate
29 Randolph Rd
AIR FORCE MATERIEL COMMAND
Hanscom AFB, MA 01731-3010

REPORT DOCUMENTATION PAGE

Form Approved
OMB No. 0704-0188

1. AGENCY USE ONLY *(Leave blank)*	2. REPORT DATE	3. REPORT TYPE AND DATES COVERED
	1 Nov 1999	Final, 8 Nov 1991-30 Sep 1998

4. TITLE AND SUBTITLE
Mesoscale Ionospheric Phenomena

5. FUNDING NUMBERS
PE 61102F
PR 2310
TA G6
WU EA

Contract F19628-91-K-0043

6. AUTHOR(S)
Tom Chang

7. PERFORMING ORGANIZATION NAME(S) AND ADDRESS(ES)
Massachusetts Institute of Technology
Center for Space Research
Center for Theoretical Geo/Cosmo Plasma Physics
Cambridge, MA 02139

8. PERFORMING ORGANIZATION REPORT NUMBER

9. SPONSORING/MONITORING AGENCY NAME(S) AND ADDRESS(ES)
Air ForceResearch Laboratory/VSBS
29 Randolph Rd
Hanscom AFB, MA 01731-3010
Contract Manager: Bamandas Basu

10. SPONSORING/MONITORING AGENCY REPORT NUMBER
AFRL-VS-TR-1999-1537

11. SUPPLEMENTARY NOTES
Ion Energization and Outflow was reprinted from Physics of Space Plasmas, (1998) No. 15, pp 15-20; The Role of Self-Organzed Criticality . . . from pp 61-66 of the same journal and issue, and New Results of the Theory of Non-Classical Polar Wind from pgs 319-324 of the same journal and issue.

12a. DISTRIBUTION AVAILABILITY STATEMENT
Approved for public release; Distribution unlimited

12b. DISTRIBUTION CODE

13. ABSTRACT *(Maximum 200 words)*

Results of a seven-year study of a variety of multiscale plasma processes in the ionosphere and magnetosphere are described. Specific topics discussed in detail include: (1) ion energization and outflow; (2) self-organizad criticality and multiscale intermittent turbulence in the plasma sheet; and (3) a new theory of the nonclassical polar wind. A complete listing of published papers and books during the years 1992-1998 is also included.

14. SUBJECT TERMS
Ion conics, Turbulence, Polar wind, Self-organized criticality, Plasma sheet, Particle acceleration.

15. NUMBER OF PAGES
36

16. PRICE CODE

17. SECURITY CLASSIFICATION OF REPORT	18. SECURITY CLASSIFICATION OF THIS PAGE	19. SECURITY CLASSIFICATION OF ABSTRACT	20. LIMITATION OF ABSTRACT
UNCLASSIFIED	UNCLASSIFIED	UNCLASSIFIED	SAR

TABLE OF CONTENTS

1. SYNOPSIS OF CONTRACT ACTIVITIES

During the past seven years, we have made substantive contributions toward the goals set forth in our original grant proposal. In the research area, we have succeeded in developing the basic understanding of several mesoscale space plasma phenomena of considerable importance. These include the study of the origin of high-latitude magnetospheric-ionospheric turbulence, the formation of ion conics in the auroral and cusp regions, the generation of counterstreaming electrons along auroral field lines, the process leading to the anomalous heat transport in the polar wind due to photoelectrons, the development of black auroral curls in the return current region, the apparent low-dimensional behavior of self-organized criticality and global geomagnetic activity, and other related nonlinear space plasma processes. A number of these theoretical findings have recently been confirmed by experimental data collected by high-time resolution instruments on board the Freja, Akebono, POLAR and FAST satellites as well as the TOPAZ, SCIFER and AMICIST rocket series. As a gauge of the seminal nature and excellence of our contributions and their popular acceptance by our peers, we note that we were invited to deliver a total of over 50 invited and review lectures at various national and international conferences and major prestigious institutions. We were also asked to chair and/or organize specialty sessions on particle acceleration, polar wind and multiscale phenomena at a number of conferences and workshops. During the contract period, we published a total of 40 scientific papers and five proceedings volumes.

We have interacted with a number of research organizations including the Air Force Research Laboratory, the Naval Research Laboratory, Cornell University, the

International Space Science Institute, the Universities of California at Berkeley, Los Angeles and Irvine, the University of Maryland, the University of New Hampshire, Boston College, the Max-Planck Institutes for Extraterrestrial Physics and Aeronomy, the Lockheed Palo Alto Research Laboratory, the National Research Council of Canada, the University of Iowa, the Swedish Space Institute and the Space Research Institute in Moscow. Visits to these institutions and by scientists from these institutions have provided the necessary stimulus to keep our research program vibrant, up-to-date, and at the same time constantly in touch with practical motivations.

We organized several combined Symposia/Workshops on the "Physics of Space Plasmas" covering the topics of "Chaos, Stochasticity, and Strong Turbulence." and "Multiscale Phenomena in Space Plasmas." In addition, Dr. Tom Chang organized a Memorial Symposium for the Nobel Laureate, Professor S. Chandrasekhar of the University of Chicago. This activity was held in conjunction with the Annual Meeting of the Society of Engineering Science in October 1996 at the Campus of the Arizona State University in Tempe. This event attracted over 300 scientists and engineers world-wide.

The content of this report is organized as follows. In Sections 2 - 4, we discuss in detail the three most noteworthy contributions of our research activities: (1) ion energization and outflow, (2) self-organized criticality and multiscale intermittent turbulence in the plasma sheet, and (3) a new theory of the nonclassical polar wind. In Section 5, a complete listing of the scientific publications of the MIT group during the contract period (including the titles of five edited conference proceedings) is provided.

Ion Energization and Outflow: Some Important Mechanisms

Mats André and Patrik Norqvist

Swedish Institute of Space Physics, Department of Theoretical Space Physics, Umeå University, 901 87 Umeå, Sweden

Tom Chang

Center for Space Research, Massachusetts Institute of Technology, Cambridge, MA 02139, USA

Abstract. More than one mechanism is causing ion energization perpendicular to the geomagnetic field in the terrestrial auroral region. Ions energized in this way may leave the ionosphere, and are an important source of magnetospheric plasma. Observations by the Freja satellite obtained during 20 months at altitudes around 1700 km are used to study the most common O^+ energization mechanisms. The most common and most important ion energization is due to broadband low-frequency waves, causing resonant energization by interaction at frequencies around the ion gyrofrequency. This mechanisms is compared with other types of ion energization. The dependence of the different energization types on magnetic local time and magnetic latitude is presented. We also speculate on the origin of the broadband waves causing most of the ion energization.

1. Introduction

An intriguing problem of magnetospheric physics is the energization of ionospheric ions and their subsequent escape from low altitudes. Much of the ion outflow is caused by ion heating in the direction perpendicular to the geomagnetic field. The heated ions may then move up the field lines of the inhomogeneous terrestrial magnetic field and form so-called conics in velocity space. This ion energization is often associated with the auroral region and occurs at all local times. Several ion energization mechanisms have been suggested, but the relative importance of the different mechanisms has not previously been established. Using observations of O^+ ions obtained by the Freja satellite, we present a statistical study of the most common O^+ ion energization mechanisms.

Observations of perpendicular ion heating have been obtained during several years from rockets and satellites at altitudes from a few hundred kilometer and at least up to several Earth radii. The ion distributions may have average energies from a few eV up to at least a few keV, i.e., thousands of times higher than the mean ion energies in the lower ionosphere. Most of the energization takes place above the collisional ionosphere and thus depends on interaction between the charged ions and some electric fields. The importance of ionospheric ion outflow as a source of magnetospheric plasma is well established by statistical studies using polar orbiting satellites, as discussed in reviews by *Moore and Delcourt* [1995] and *Yau and André*, [1997]. Several ion energization mechanisms causing this outflow have been suggested (see reviews by, e.g., *Klumpar*, 1986; *Lysak*, 1986, *André and Chang*, 1993; *André*, 1997; *André and Yau*, 1997; *Chang and André*, 1998)

Recent observations indicate that more than one ion energization mechanism is operating in the terrestrial auroral region, but also suggest that one mechanism is the most important. Broadband low-frequency electric wave fields are commonly observed together with perpendicular ion energization. These waves cover frequencies from below one Hz up to several hundred Hz, thus including the gyrofrequencies of the major ion species at least for altitudes from about 1000 km up to several Earth radii. Several wave and particle observations by satellites [e.g., *Norqvist et al.*, 1996; *Carlson et al.*, 1998] and by rockets [e.g., *Lynch et al.*, 1996; *Kintner et al.*, 1996] indicate a clear correlation between these waves and ion energization. Resonant energization by the observed waves at frequencies near the ion gyrofrequency usually can heat the ions to the observed energies [*Chang et al.*, 1986; *Retterer et al.*, 1987; *Jasperse*, 1998]. In the following we give an overview of some recent statistical studies of observations obtained by the Freja satellite. We conclude that resonant heating by broadband low-frequency waves is the dominating ion energization mechanism.

2. An Example of Ion Energization Observed by the Freja Satellite

The Freja satellite was launched October 6, 1992, into an orbit with 63° inclination, an apogee in the northern hemisphere of 1750 km, and a perigee of 600 km. The Freja instruments include the TICS ion mass

spectrometer, the TESP electron spectrometer, experiments for observing low frequency electric and magnetic fields, and experiments for electric and magnetic wave fields and the plasma density. The Freja instruments are described in *Space Science Reviews, 70,* 405–602, 1994. Observations by Freja have been used to define a few different types of ion energization. Below we present an example of an ion energization event.

An intense morningside ion heating event occurred on December 3, 1993, on orbit 5591. The corrected geomagnetic latitude (CGL) was about 72°, the magnetic local time (MLT) was around 0600, and the *Kp* index was 5. Figure 1 shows an overview of the observations (see also *Eliasson*, [1996] and *André et al.*,[1998]). Note that Freja is moving essentially tangential to the auroral oval (at nearly constant CGL) during the event.

Oxygen ion count rates from the TICS ion mass spectrometer are shown in panel 1 of Figure 1. The corresponding pitch angles are displayed in panel 3. Heated ions can be seen as vertical stripes in panel 1 between 0842:10 and 0842:30, and also between 0843:10 and 0844:55 UT. It is the heating of these O^+ ions we consider. Panel 2 shows data from the TICS proton channel, which is not used in our statistical studies.

Panel 4 displays downgoing electrons observed by the TESP detector. Note that the downgoing keV (so-called inverted V) electrons are anticorrelated with the ion energization. We have found that during several events, on a timescale of minutes (several hundreds of kilometers along the satellite trajectory) the ion heating and keV auroral electrons are associated, but on a timescale of seconds (tens of kilometers) the ion energization and the auroral electrons are anticorrelated.

Panel 6 shows a time series of the perpendicular low-frequency (below tens of Hz) electric field in the satellite spin plane, while panel 8 displays a time series of the low-frequency magnetic field fluctuations. The amplitude of these electric and magnetic fluctuations are correlated with the O^+ ion energization.

Panel 5 displays an electric field spectrum up to 16 kHz. There is a good correlation between waves with frequencies from below one hertz up to several times the oxygen gyrofrequency f_{O+} at 25 Hz and the ion heating. There are also some waves in the lower hybrid frequency range (1 to 2 kHz), but there is no detailed correlation with the ion heating. Panel 7 shows a spectrum of the magnetic field below 64 Hz. The magnetic spectral density is also correlated with the ion heating. However, the magnetic spectrum decreases more rapidly with increasing frequency than the electric spectrum. Panel 9 displays the density, obtained from a Langmuir probe.

To summarize, a clear correlation between the transversely heated oxygen ions and waves with frequencies from below one hertz up to several times f_{O+} is observed for this event. It can be shown that generally the observed wave amplitudes are high enough to heat the O^+ ions to the observed energies for such events [*André et al.*, 1998].

3. Different Types of Ion Energization

By considering in detail data sets obtained by Freja during 20 events at various local times, a few different types of ion heating events can be defined. An example of a data set is shown in Figure 1.

Type 1 ion heating is by *Norqvist et al.* [1998] defined to be associated with broadband low-frequency waves, similar to the event in Figure 1. An increase of the field-aligned current is often associated with this type of ion heating. The heating may also be associated with suprathermal electron bursts, i.e., field aligned electrons covering a broad energy range from tens of eV up to several hundred eV.

Type 2 ion heating is also associated with broadband low-frequency waves, although the ratio of the electric and magnetic field is typically smaller than for type 1 events. These events are associated with precipitating protons with keV energies, and electrons with mean energies of about 100 eV, typical of the cusp/cleft region. Similar to type 2 events, type 1 events are often associated with field-aligned currents, and with suprathermal electron bursts.

Type 3 ion heating is associated with downgoing keV auroral electrons. Type 3(LH) events are associated with waves near the lower hybrid frequency, while type 3(EMIC) are associated with electromagnetic ion cyclotron waves at about half the proton gyrofrequency.

4. A Statistical Study of Ion Energization Mechanisms

Using Freja observations obtained in the northern hemisphere from late January 1993 to the middle of September 1994, a statsitical study of ion energization mechanisms has been performed [*Norqvist et al.*, 1998]. This period coincides with the declining phase of solar cycle 22. The corrected geomagnetic latitude (CGL) of the events is from about 50° to 75°, the upper limit being set by the 63° degree inclination of the orbit. Essentially all observations are obtained between 1400 and 1750 km, with a majority of the observations ocurring around 1700 km.

Since some of the upward flowing ions may come back to low altitudes, we use the term upflow, rather than outflow, in the following. This upflow is calculated as upward ion flux minus downward ion flux, and the flux is corrected for the satellite motion parallel to the geomagnetic field. The upflow is normalized with respect to the total number of satellite spins in the appropriate bin, using zero flux for spins not regarded as an event. Finally the upflow is projected to a reference altitude of 1000 km.

Useful data were obtained from about 700 000 six second spacecraft spins, of which about 500 000 occurred at invariant latitudes above 60°. In the following statistics, ion energization of types 3(LH) and 3(EMIC) are treated together as type 3. The relative importance of lower hybrid and EMIC waves is discussed in section

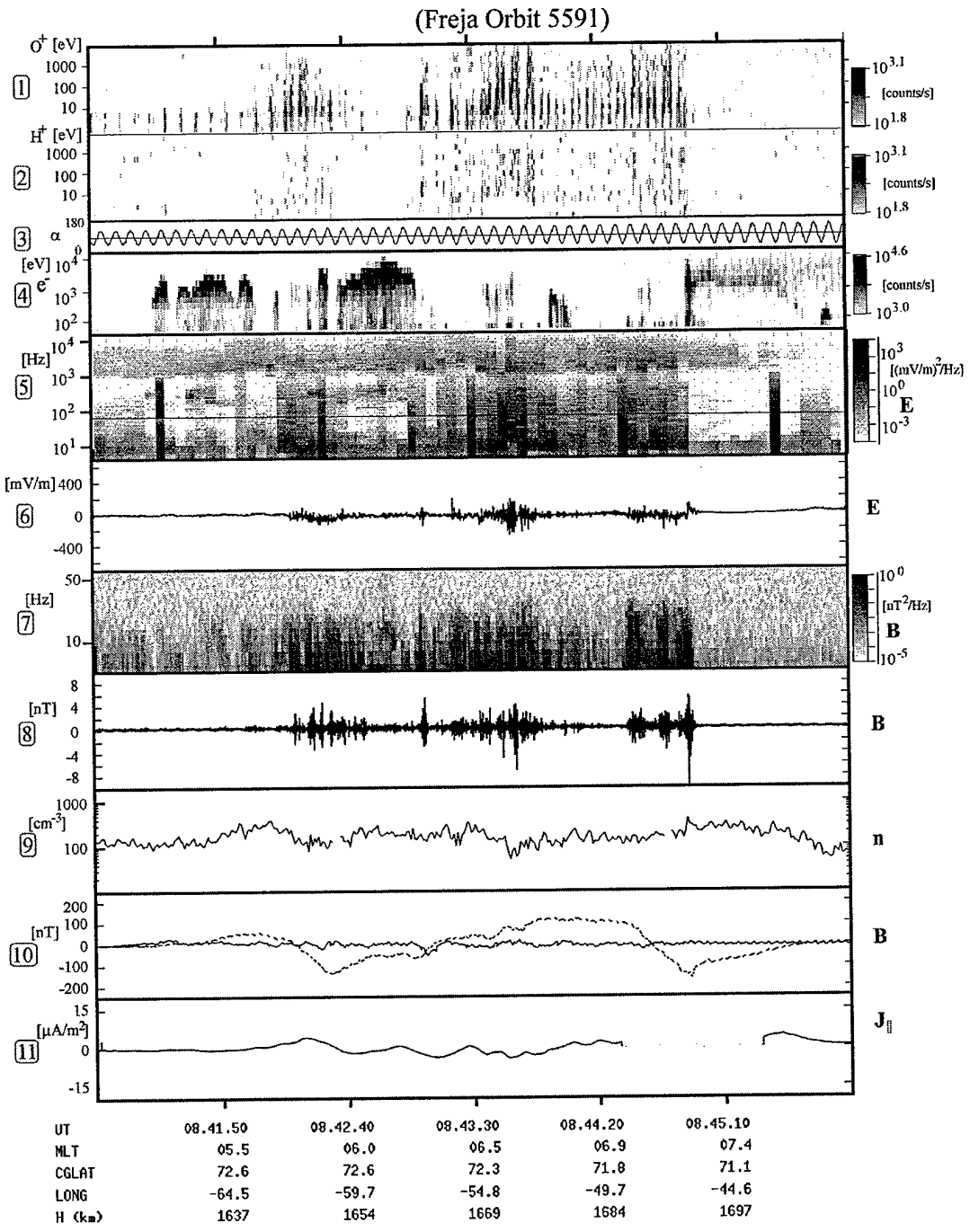

Figure 1. Freja data from December 3, 1993 when the satellite passed a morningside ion heating region of type 1. The data in the various panels are discussed in the text. There is a good correlation between the electric and magnetic wave fields in panels 5 and 7, and the O^+ ion energization in panel 1. (From *André et al.* [1998].)

5. A total of 5211 spins with heated O^+ ions includes 3358 (64.4 %) of type 1, 1213 (23.3 %) of type 2, and 640 (12.3 %) of type 3. As demonstrated later, type 2 is associated with higher upflow and also dominates the total upflow.

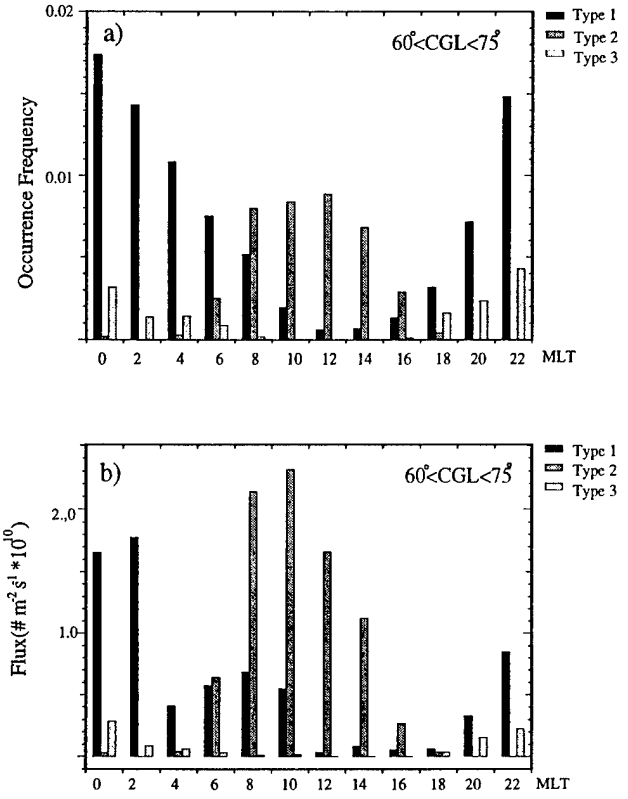

Figure 2. a) Occurrence frequency for the three ion heating types versus MLT. b) The corresponding average upward O^+ flux (averaging include all samples with zero upward flux) projected to an altitude of 1000 km. Type 1 dominates the nightside, while type 2 is most common on the dayside. Both types are caused by broadband low-frequency waves, and together completely dominate the total O^+ upflow. (From *Norqvist et al.* [1998].)

The occurrence frequency for oxygen heating events of type M, f_M, we define as

$$f_M(i,j) = \frac{n_M(i,j)}{N(i,j)} \qquad (1)$$

where n_M is the number of samples (satellite spins) of type M events and N is the total number of samples in a specific bin. The binning parameters (MLT, CGL) are denoted i and j. At the altitude and latitude of our study the difference between CGL and INVL (used in the invariant geomagnetic dipole coordinate system) is small, and can be neglected. In the data presentation, summation of one of the indices is performed. This summation is made over all values of the binning parameter if nothing else is stated.

4.1. Magnetic Local Time Dependence

The occurrence frequency of each heating type as a function of magnetic local time for CGL>60° is shown in Figure 2a. Type 1 is the most common heating type on the nightside. These events are distributed around midnight with a slight predominance on the morningside. Type 2 is the most common energization type around noon. These events are significantly more common in the prenoon sector, as compared to the postnoon sector. The type 3 events are mainly found at the nightside. These events are clearly more common on the evening side than on the morningside.

The average O^+ upflow (upward number flux) as a function of MLT for all three heating types, is shown in Figure 2b. Type 2 events in the prenoon sector give the highest upward O^+ flux. One reason that type 2 on the dayside dominate the upflow, although type 1 on the nightside has higher occurrence frequency, is that the plasma density is higher on the dayside. The average upflow during a spin regarded as an event can be obtained by dividing the upflow in Figure 2b with the occurrence frequency in Figure 2a. Thus, the average O^+ upflow during a prenoon event is a few times $10^{12}/(m^2s)$, but large upflows can be at least ten times higher [*André et al.*, 1998]. A maximum particle upflow in the prenoon sector agrees with many previous studies, [see e.g., *Lockwood et al.*, 1985]. About 90 % of the events in Figure 3 are of type 1 or 2, and about 95 % of the O^+ upflow is related to these events. Since the type 1 and 2 are associated with broadband low-frequency waves, we find that most of the ion upflow is caused by these waves.

4.2. Magnetic Latitude Dependence

The occurrence frequency of each heating type as a function of corrected magnetic latitude is shown in Figure 3a. Type 1 has a peak in occurrence frequency around 70°, and type 3 peaks at slightly lower latitudes. In contrast, the occurrence frequency of type 2 increases up to 75°, the highest latitude included in the study, indicating a maximum at even higher latitudes. The upflow in Figure 3b shows a dependence on latitude similar to that of occurrence frequency for all types. The peak in upflow associated with type 1 ion heating at 62° is caused mainly by data from a single orbit with many spins of high density conics, and is believed not to be statistically significant. As in Figure 2b we find that the highest upflows are caused by type 2 ion heating. An upflow increasing with latitude in Figure 3b is consistent with results from the DE-1 satellite which show a peak in upward O^+ flux near noon, where type 2 events dominate, around 78° (Figure 8 of *Yau et al.* [1985]). However, the DE-1 peak flux near midnight, where type 1 and type 3 events dominate, is just below 70°, again consistent with Figure 3b.

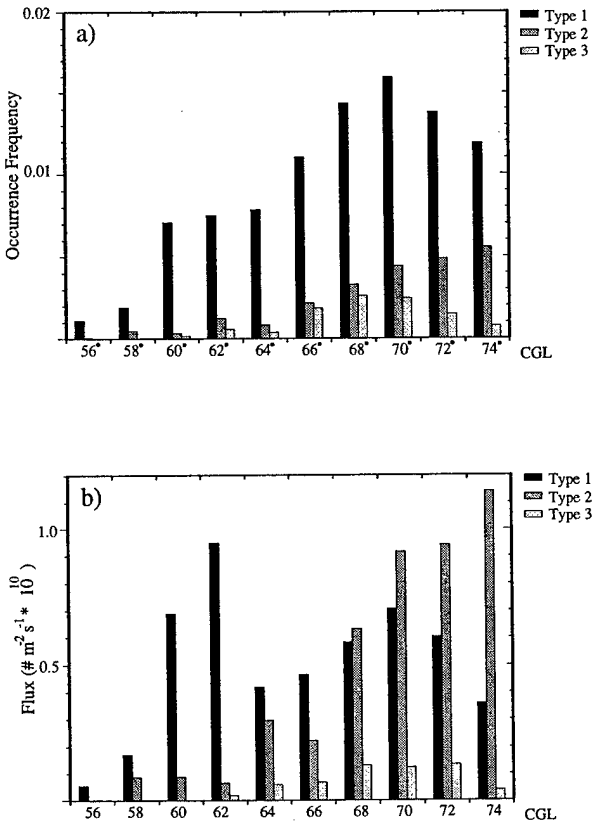

Figure 3. a) Occurrence frequency, and b) upflow associated with three ion heating types, as a function of Corrected Geomagnetic Latitude. (From *Norqvist et al.* [1998].)

4.3. Associated Electron Energy

The energy flux of field-aligned downgoing electrons in and near regions of ion energization were studied by *André et al.* [1998]. During type 1 events (e.g., Figure 1) it is clear that high electron energies are found near, but outside, the intense ion energization. Figure 4a shows an anticorrelation of electron energy flux and ion energy. Recent observations by the FAST satellite show that very field-aligned electron beams reaching energies of hundreds of eV may be common in type 1 ion heating regions [*Carlson et al.*, 1998]. Some of these very field-aligned particles may sometimes be missed by the Freja detectors, but their mean energy is typically lower than that of auroral electrons detected nearby. During type 3 events, high electron energy fluxes are found to be directly associated with the ion energization, Figure 4b. The relation between the electron fluxes and the waves causing the ion energization is discussed below.

5. Waves Associated with Ion Energization

We first consider the waves associated with type 3 events. It is clear that waves near the lower hybrid frequency, and also EMIC waves at about half the proton gyrofrequency, can be generated by downgoing keV auroral electrons [e.g., *Chang and Coppi*, 1981; *Vaivads et al.*, 1998]. In about 60 % of the type 3 events studied by *Norqvist et al.* [1998], lower hybrid waves seem to have higher amplitude than all other types of waves (type 3(LH) events). In about 20 % of the events, EMIC waves are the most intense emissions (type 3(EMIC)). For the remaining 20% of the O^+ heating events, broadband low-frequency waves have the highest amplitudes. This means that the statistics of type 3 events really gives an upper limit of the importance of EMIC emissions and waves near the lower hybrid frequency.

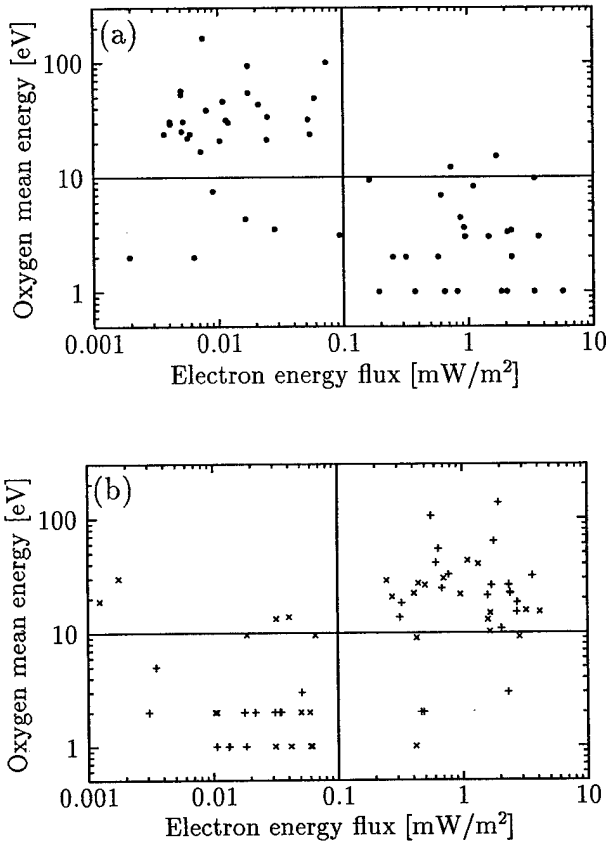

Figure 4. Mean O^+ energy as a function of energy flux of auroral electrons for (a) type 1 events and (b) type 3 events. For type 1 the O^+ energy is anticorrelated with the auroral electrons when studied on timescales of a few seconds, while for type 3 the O^+ energy is correlated with the auroral electrons. (From *André et al.* [1998].)

For type 1 and 2 events, broadband low-frequency waves dominate the ion energization. The energy transfer from the waves to the ions can be modeled and it can be shown that the wave amplitudes are high enough to cause the observed ion energies [e.g., *André et al.*, 1998]. However, the origin of the waves is not understood. One possibility is that the braodband waves contain a small fraction of left-hand polarized electromagnetic component (either locally generated or propagated there), which can gyroresonantly energize the ions [*Chang et al.*, 1986].

Alternatively, essentially electrostatic waves near the ion gyrofrequency could be generated by a field-aligned current in a homogeneous plasma carried by a drifting electron distribution [*Kindel and Kennel*, 1971]. Using reasonable assumptions, *André et al.*, [1998] showed that the observed currents are not high enough to generate waves in this way. Also, according to simple theory, the waves that would be generated by higher current densities might not be as broadband as the observed emissions. Field-aligned electron beams with higher energies (up to hundreds of eV) may have velocities matching the local Alfvén speed, When these beams have high enough densities they may generate more electromagnetic waves. However, as for the electrostatic emissions, these waves would according to simple theory not be as broadband as the observed emissions.

An interesting possibility to decrease the current needed to generate waves, and to obtain more broadband emissions, is to introduce gradients perpendicular to the geomagnetic field in the model [*Ganguli*, 1997; and references therein]. Laboratory experiments using parameters relevant for space plasmas confirm that gradients in perpendicular electric fields decrease the current needed for wave generation, and that rather broadband waves can be obtained [*Amatucci et al.*, 1996; *Koepke et al.*, 1998; and references contained therein]. A possible scenario in type 1 and 2 ion energization regions is that a downward propagating Alfveń wave with frequency of around 1 Hz provides a gradient in the perpendicular electric field. A rather small field-aligned current can then generate fairly broadband waves. However, this scenario is hard to immediately confirm from observations. It is not clear how meaningful it is to split the measured broadband wave spectrum into one part much below the ion gyrofrequency (the Alfvén wave generated somewhere else, providing electric field gradients) and a more broadband part around the ion gyrofrequency (locally generated by the large scale current, in the presence of the electric field gradients). The latter part would then energize the ions. A starting point for a detailed investigation could be the fact that the ratio of the electric and magnetic fields of the broadband waves often is more consistent with Alfvén waves at the lowest frequencies, as compared with the more electrostatic emissions at higher frequencies.

6. Summary

More than one ion energization mechanism is operating in the terrestrial auroral region. Using Freja observations from altitudes near 1700 km in the auroral region, we conclude that resonant energization by broadband low-frequency waves is the most important mechanism for the energization and outflow of O^+ ions. This mechanism dominates the O^+ outflow at all local times, and at all levels of magnetic activity. Resonant energization by waves near the lower hybrid frequency, and by EMIC waves, occurs in the pre-midnight and midnight sectors. These mechanisms may dominate specific events, but give lower total outflow as compared to energization by broadband low-frequency waves.

Acknowledgments We are grateful to the Freja principal investigators Manfred Boehm, Lars Eliasson, Bengt Holback, Göran Marklund and Larry Zanetti for supplying data to our studies. A portion of this research was supported by AFOSR, AFRL, NSF.

References

Amatucci W.E., *et al.*, *Phys. Rev. Lett.*, **77**, 1978, 1996.

André, M., *J. Atmos. Terr. Phys.*, **59**, 1687, 1997.

André, M., *et al.*, *J. Geophys. Res.*, **103**, 4199, 1998.

André, M., and T. Chang, *Physics of Space Plasmas (1992)*, **12**, 35, 1993.

André, M., and A.W. Yau, *Space Sci. Rev.*, **80**, 27, 1997.

Chang, T., *et al.*, *Geophys. Res. Lett.*, **13**, 636, 1986.

Chang, T., and B. Coppi, *Geophys. Res. Lett.*, **8**, 1253, 1981.

Chang, T., and M. André, in *Geospace Mass and Energy Flow, Geophys. Monogr. Ser.*, **104**, edited by J.L. Horwitz *et al.*, 115, AGU, Washington, D.C., 1998.

Carlson, C.W., *et al.*, *Geophys. Res. Lett.*, **25**, 2017, 1998.

Eliasson, L., *Adv. Space Res.*, **8**, 85, 1996.

Ganguli, G., *Phys. Plasmas*, **4**, 1544, 1997.

Jasperse, J.R., *Geophys. Res. Lett.*, **25**, 3485, 1998.

Kindel, J.M., and C.F. Kennel, *J. Geophys. Res.*, **76**, 3055, 1971.

Kintner, P.M., *et al.*, *Geophys. Res. Lett.*, **23**, 1873, 1996.

Klumpar, D.M., in *Ion Acceleration in the Magnetosphere and Ionosphere, Geophys. Monogr. Ser.*, **38**, edited by T. Chang, 389, AGU, Washington, D.C., 1986.

Koepke, M.E., *et al.*, *Phys. Rev. Lett.*, **80**, 1441, 1998.

Lockwood, M., *et al.*, *J. Geophys. Res.*, **90**, 4099, 1985.

Lynch, K.A., *et al.*, *Geophys. Res. Lett.* **23**, 3293, 1996.

Lysak, R.L., in *Ion Acceleration in the Magnetosphere and Ionosphere, Geophys. Monogr. Ser.*, **38**, edited by T. Chang, 261, AGU, Washington, D.C., 1986.

Moore, T.E., and D.C. Delcourt, *Reviews of Geophysics*, **33**, 175, 1995.

Norqvist, P., *et al.*, *J. Geophys. Res.*, **101**, 13179, 1996.

Norqvist P., M. André, and M. Tyrland, *J. Geophys. Res.*, 103, 23459, 1998.

Retterer, J. M., *et al.*, *Phys. Rev. Lett.*, **59**, 148, 1987.

Vaivads, A., *et al.*, *J. Geophys. Res.*, in press, 1998.

Yau, A. W. and M. André, *Space Sci. Rev.*, **80**, 1, 1997.

Yau, A. W., *et al.*, *J. Geophys. Res.*, **90**, 8417, 1985.

The Role of Self-Organized Criticality and Multiscale Intermittent Turbulence in Magnetotail Dynamics

Tom Chang

Center for Space Research, Massachusetts Institute of Technology, Cambridge, MA 02139, USA, and International Space Science Institute, Bern, Switzerland

Abstract. It is shown that self-organized criticality and multiscale intermittent turbulence characterize the underlying physics of the substorm behavior of the Earth's magnetotail. The model incorporates a multitude of cross-scale interactions of coherent structures and plasma fluctuations. Such a description provides a convenient explanation of the localized and sporadic nature of the reconnection signatures (bursty bulk flows) that are commonly observed in the tail region of the magnetosphere [*Angelopoulos et al.*, 1996; *Lui*, 1998, and references contained therein]. The onset of substorm is then attributed to the emergence of a global nonclassical nonlinear instability characterized by the enhanced mixing and merging of the coherent structures, leading to the phenomenon of self-organized criticality (SOC) with low-dimensional chaotic signatures and fractal behavior. These concepts provide a new paradigm for the understanding of the ever-elusive phenomenon of magnetic substorms.

1. Synopsis

In-situ experimental observations [*Angelopoulos et al.*, 1996; *Lui*, 1998, and references contained therein] and simulations [*Drake*, 1997; *Büchner*, 1998] indicate that the magnetotail dynamics associated with substorms are intermittent and turbulent. A model involving the generation, dispersing, and merging of multiscale coherent plasma structures and fluctuations is suggested to address the implications of such observations [*Chang*, 1998].

The merging of localized coherent structures during such a dynamic process are shown to be responsible for the commonly detected sporadic reconnection signatures and associated plasmoids in the magnetotail and contribute to the origin of the observed "bursty bulk flows".

The commencement of a substorm is relegated to the onset of a global nonclassical nonlinear instability, signaled by the enhanced mixing and merging of coherent structures and other plasma fluctuations. The ensuing substorm dynamics is then postulated to be characterized by the phenomenon of self-organized criticality (SOC).

Using its invariance properties, it has been shown by *Chang* [1992], that systems near self-organized criticality will generally acquire the characteristics of low dimensionality and fractal structures; thus providing a rationale for the conjectured chaotic behavior of substorm dynamics based on finite-dimensional nonlinear dynamics arguments [*Baker et al.*, 1990; *Vassiliadis et al.*, 1990; *Klimas et al.*, 1992; *Sharma et al.*, 1993; *Klimas et al.*, 1998].

This leads us to consider the fluctuation spectra for the inhomogeneous, anisotropic intermittent turbulent plasma medium of the magnetotail during substorms. The concept of multifractals is then introduced and related to the scaling regions of the spectra for coherent, MHD and kinetic states. Recent observations seem to validate the above hypothesis [*Hosino et al.*, 1997; *Milovanov et al.*, 1996; *Zelenyi et al.*, 1998].

We will conclude by making a few suggestions with regard to the future directions of observational, laboratory and theoretical research, that might help to elucidate the detailed dynamics of this proposed new paradigm.

2. Plasma Resonances and Coherent Structures

Measurements of reconnection signatures in the "neutral sheet" region of the Earth's magnetotail indicate that most of the individual localized merging processes occur at intermediate or microscales. On the other hand, the dimensions of the full dynamic domain that is responsible for the transferring of energy and momentum from the solar wind to the Earth's magnetotail generally involve time and spatial scales much larger than those characterized by the microscopic plasma parameters such as the ion gyroradius, skin depth, Debye length, and ion cyclotron, lower hybrid or plasma frequencies. The transport processes at the two ends of the dynamic spectrum can involve characteristic parameters differ by orders of magnitude, suggesting that the underlying dynamics of the magnetotail is intrinsically multiscale.

Thus, we adopt a middle of the road approach in viewing the magnetotail by assuming that the dynamics of the plasma medium is primarily characterized by the basic MHD variables with an anisotropic pressure

MIT Center for Theoretical Geo/Cosmo Plasma Physics, Cambridge, MA

tensor. To bring in some of the possible kinetic effects, we can, e.g., relate the pressure tensor to the particle distribution functions $f_i(\mathbf{x}, \mathbf{v}, t)$ in terms of the appropriate moments.

$$\mathbf{P} = \sum_i m_i \int (\mathbf{v} - \mathbf{V})(\mathbf{v} - \mathbf{V}) f_i(\mathbf{v})\, d\mathbf{v} \qquad (1)$$

where $f_i(\mathbf{x}, \mathbf{v}, t)$ satisfy the Vlasov equations.

Standard arguments lead to the following coupled equations of induction and motion:

$$d\mathbf{B}/dt = (\mathbf{B} \cdot \nabla)\mathbf{V} + \ldots, \; and \qquad (2)$$

$$\rho\, d\mathbf{V}/dt = (\mathbf{B} \cdot \nabla)\mathbf{B} + \ldots, \qquad (3)$$

where all notations are customary and the ellipsis represent compressibility, and anisotropic pressure effects. Generally, of course, dissipative terms must also be included. It is clear from above that one of the wave modes allowed by these equations is the shear Alfvén wave. For such modes to propagate, the propagation vector $\mathbf{k}$ must contain a field-aligned component, i.e., $\mathbf{B} \cdot \nabla \rightarrow i\mathbf{k} \cdot \mathbf{B} \neq 0$. However, at sites where the parallel component of the propagation vector vanishes, $k_{\|} = \mathbf{k} \cdot \mathbf{B} = 0$, energies are localized and the field lines may be distorted effortlessly. These singularities (points, curves or surfaces) at which $k_{\|} = 0$ are called "shear Alfvén resonances". As it will be demonstrated below, the existence of shear Alfvén resonances will lead to the formation of nearly-nonpropagating and essentially closed macroscopic magnetic structures.

We now consider the magnetic field structures near the Alfvén resonances. Neglecting the pressure effects, it is clear from Eqs. (2), (3) that the forces arise from the fluctuations just away from these singular (resonance) sites, i.e., $\delta\mathbf{B} \cdot \nabla$, will tend to restore the field lines towards the resonance sites, thereby forming essentially closed coherent magnetic structures. In the following we shall consider the general topology of such coherent structures.

For an ideal MHD system, any physically acceptable magnetic field must satisfy $\nabla \cdot \mathbf{B} = 0$. Also, any variation of the field away from the initial value must satisfy the constraint:

$$\partial\mathbf{B}/\partial t = \nabla \times (\mathbf{v} \times \mathbf{B}). \qquad (4)$$

Taylor [1974] demonstrated that Eq. (4) may be replaced by an infinite set of integral constraints involving the *helicity* K, such that

$$K = \int_V \mathbf{A} \cdot \mathbf{B}\, dV \qquad (5)$$

is an invariant for any volume V enclosed by a flux surface, where $\mathbf{A}$ is the vector potential. It can be shown that as the system relaxes to its minimum energy state satisfying the helicity conservation constraints, the magnetic structure will be in a force-free state, i.e.,

$$\mathbf{j} \times \mathbf{B} = 0. \qquad (6)$$

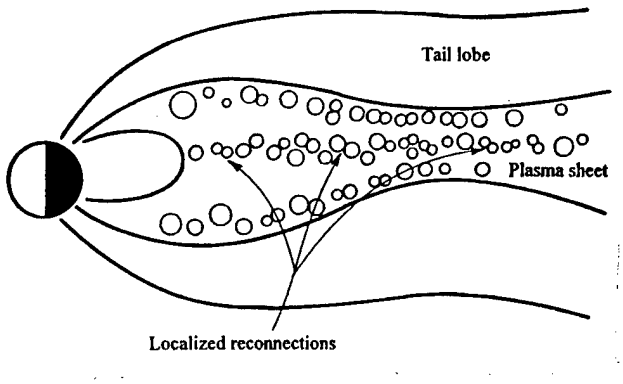

Figure 1. Cross-sectional view of sporadically distributed flux tubes in the plasma sheet.

Taylor's Conjecture and Coarse-Grained Helicity. Let us now consider our present situation at hand. We are interested in the more realistic situation that characterizes the dynamics of the magnetotail where the plasma is slightly dissipative and in addition, there are stochastic macroscopic (as well as microscopic) fluctuations. The dissipation and magnetic stochasticity will allow the field lines to merge, mix, and break. It is obvious that it no longer makes sense to discuss the topology of individual field lines. Nevertheless, it was suggested by *Taylor* [1974] that when the volume integral for Eq. (5) is taken over the "stochastic region", the coarse-grain averaged helicity will be essentially conserved. This indicates that when considering the stochastic domain, the average magnetic structure in a relaxed state will again be essentially force free, with $\mathbf{j} \times \mathbf{B} = 0$, where $\mathbf{j}$ and $\mathbf{B}$ are now to be interpreted as the mean current and magnetic field, respectively. This result can also be arrived at using the clump theory of MHD turbulence [*Tetreault*, 1992, and references contained therein].

We are, of course, interested in the magnetotail at dynamic states that are far from equilibrium. Thus, in visualizing the relaxed states from the point of view of the Taylor's conjecture, we shall consider timescales such that "nearly coherent" magnetic structures are formed.

Let us now apply these concepts to the sheared magnetic field geometries that are generally found in the "neutral sheet" region of the magnetotail. The nearly force-free condition for the coarse-grain averaged coherent structures would then orient themselves more-or-less in the average cross-tail current direction in the form of twisted flux tubes. In general, there will be a constellation of such coherent structures immersed in the turbulent plasma medium, Fig. 1.

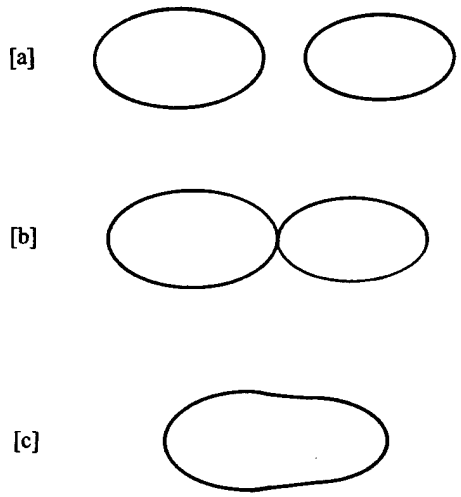

Figure 2. Cross-sectional view of coherent structures at various stages of merging. (a) Just Prior to Merging. (b) During the process of merging. (c) Relaxed state after merging.

3. Stochastic Merging of Coherent Structures

As the coherent structures migrate toward each other, they will merge and form new coherent structures. Depending on the polarities and intensities of the currents that orient these flux tubes, the resulting coherent structures will be either larger or smaller than the original individual structures. The final states of the new coherent structures will again be essentially force-free in the coarse-grained sense. As these new structures are generated, new MHD fluctuations are produced; and thereby spontaneously set up new resonance sites. Thus, an interesting scenario of intermittent turbulent mixing, diffusing, and merging sets in.

Let us consider the most probable situation of merging, i.e., the merging of two coherent structures. Viewed in a section normal to the average direction of the cross-tail current, the topologies of the field lines during such a merging process mimic that is generally considered for a classical magnetic "reconnection" process [Fig. 2]. However, we note that this localized merging process can take place without the requirement of $\mathbf{B} = 0$ and/or the existence of a true "neutral line." In fact, as seen above, the prerequisite for the existence of many such coherent structures as well as the sporadic merging of these structures is the existence of many "Alfvén resonance" sites with $k_{\|} = 0$. This occurs when the background magnetic field is three-dimensional and nonzero and when there are three-dimensional macroscopic MHD fluctuations.

Thus, we suggest that as a spacecraft flies through the neutral sheet region of the magnetotail, there is a finite probability for the instruments on the spacecraft to detect classical-like reconnection signatures. Such signatures can be detected nearly anywhere in the plasma sheet, but more probably in the "neutral sheet" region, particularly during substorm times. The duration of interaction of these observed localized merging processes should be the approximate time required for the new relaxed coherent structures to emerge and in general, would be rather sporadic. We suggest that these are the origins of the observed "bursty bulk flows" [*Angelopoulos et al.*, 1996; *Lui*, 1998; *Kivelson and Kepko*, private communication].

Most of the observed localized reconnection signatures to date seem to indicate that these localized merging processes take place in domain sizes comparable to that of the ion gyroradius, especially during substorm times. Thus, very probably most of these processes will be influenced by microscopic kinetic effects. During these dynamic processes, the ions can probably be assumed to be unmagnetized and the electrons fully magnetized and the plasma nearly collisionless. This, of course, would lead to electron-induced Hall currents. Depending on the underlying magnetic geometry (since these processes can occur at any arbitrary underlying magnetic field configuration), the relevant kinetic instability that can initiate the localized merging (or reconnection) can be any of the many recently suggested microscopic instabilities such as the collisionless tearing instability, cross-field two-stream instability [*Lui*, 1996], etc. It is very probable that the nonlinear state of merging for each of these localized reconnections again entails the phenomenon of overlapping resonances [*Galeev et al.*, 1986]. (Now these resonances will arise from the localization of microscopic fluctuations, e.g., the whistler resonances, and multiple tearing modes.)

4. The Role of Self-Organized Criticality in Substorm Dynamics

Under favorable conditions (e.g., an enhancement of the cross-tail current due to the change of certain global controlling parameters for the magnetotail), the state of the turbulence discussed in the previous sections may grow (in terms of more plasma fluctuations and larger coherent structures).

This type of instability, by definition, is genuinely "nonlinear". For the onset and growth of a classical nonlinear instability, there generally exists a prescribed minimum finite amplitude of disturbance (measured, for example, by the root-mean-square of fluctuations) beyond which the fluctuations and coherent structures can grow [Fig. 3]. During the onset of a substorm, on the other hand, it has been recognized [*Chang*, 1992] that the non-equilibrium plasma state in the magnetotail is near criticality (similar to the critical point for equilibrium liquid/gas phase transitions.) At such a dynamic state (commonly referred to as a state of self-organized criticality, SOC), the effect of the fluctuations themselves becomes an important factor in determining the critical threshold of onset and the instability is now both "nonclassical" and "nonlinear" [Fig. 3]. Such an

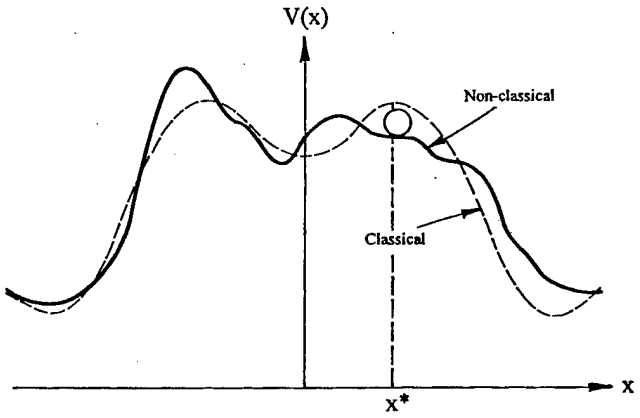

Figure 3. Marble rolling over a hill. Schematic depiction of classical and nonclassical, nonlinear instabilities. x*: Classical threshold for nonlinear instability.

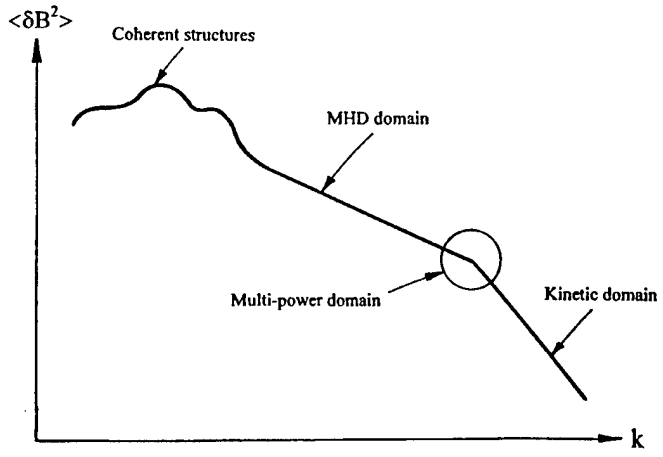

Figure 4. Fluctuation spectrum near the "neutral sheet."

instability is generally controlled by a set of relevant global parameters

The dynamics of a system at self-organized criticality is notoriously difficult to handle because the correlations of the fluctuations are long-ranged and there exist many correlation scales. On the other hand, since the correlations are extremely long-ranged, it is reasonable to expect that the system will exhibit some sort of invariance under scale transformations [*Chang et al.*, 1992; *Chang*, 1992; *Chang*, 1998].

One of the most surprising results of such theoretical arguments (based on the ideas of the dynamic renormalization-group) is that, even though the magnetotail system is infinite-dimensional and entails many, many physical parameters, its dynamics near self-organized criticality (i.e., at the onset and during magnetic substorms) can actually be characterized by a small number of relevant physical parameters (low-dimensionality). Thus, the system can be approximately described by a small number of nonlinear equations that describe the evolution of these relevant physical parameters. In addition, near criticality, these low-dimensional nonlinear equations will generally exhibit chaotic (fractal) behavior [*Chang*, 1992].

In several recent interesting papers, [*Baker et al.*, 1990; *Klimas et al.*, 1991, 1992, 1998; *Baker*, 1998], it has been suggested that certain substorm characteristics in terms of the AL time series could be modeled by deterministic chaos of simple low-dimensional dynamic equations. These results suggest that the global magnetospheric system may be "very close" to forced or self-organized criticality.

Vassiliadis et al. [1990], *Shan et al.* [1991], and *Roberts et al.* [1991] applied the technique of *Grassberger and Procaccia* [1983] for finite-dimensional systems to the AE/AL time series and estimated the dimensionally of the magnetospheric system during substorms. Their results seemed to indicate "fractals" and low-dimensional chaos.

Separately, *Sharma et al.* [1993] suggested that the dimensionality of the magnetospheric system might be obtained using the singular spectrum analysis constructed from the AE/AL time series. Their results also seemed to indicate low-dimensionality and chaos. These results appear to bestow credence to the hypothesis that substorm dynamics is indeed characterized by the phenomenon of self-organized criticality.

5. Turbulent Spectra and Multifractal Behavior

In previous sections, we demonstrated that the dynamics of the magnetotail is characterized by multiscale intermittent turbulence. A standard technique to study the behavior of such type of turbulence is through the properties of the spectra of the turbulent fluctuations.

For example, in the "neutral sheet" of the magnetotail, one of the more important spectra [Fig. 4] to consider is that of the square of the magnetic fluctuations in the cross-tail direction $\langle \delta B^2 \rangle$. We expect the spectra to generally exhibit fractal characteristics (i.e., nonclassical slopes with discernible deviations from those obtainable by naive dimensional arguments). In regions where the fluctuations and merging dimensions are much larger than that of the local ion gyroradius, the spectrum is expected to exhibit two distinguishable parts: a domain characterized by the larger scale coherent structures and a fractal domain characterized by the predominantly MHD fluctuations. On the other hand, in regions within the narrow cross-tail current sheet, we expect the spectra to exhibit at least three distinguishable parts: a domain that contains predominantly

large scale coherent structures, an MHD fractal domain and a kinetic fractal regime whose fractal dimension(s) generally depends on the type(s) of microscopic fluctuations and microinstabilities that are relevant for the merging and diffusion processes. Such type of fluctuation spectra has been recently observed [*Hosino et al.*, 1994; *Milovanov et al.*, 1996; *Zelenyi et al.*, 1998; *Lui*, 1998; and references contained therein.].

The shapes (slopes) of these spectra in the distant-tail region have been compared with results based on theoretical scaling ideas involving fractal dimensions [*Milovanov et al.*, 1996; *Zelenyi et al.*, 1998]. The difference of slopes of the various domains of an individual spectrum indicates that the scaling (fractal) behavior of each domain belongs to a different "universality class". Such type of change of scaling behavior from one universality class to another is called "symmetry breaking". In addition to the scaling properties of individual discernible domains, there are also intermediate regimes whose fractal properties are much more complicated (as indicated by the circled region of Fig. 4). The scaling laws for these regions are generally expected to exhibit multiple-power or other nonlinear characteristics [*Chang et al.*, 1992].

6. Recapitulation and Suggested New Research Directions of Magnetotail Dynamics during the Next Millennium

In summary, we have introduced a multiscale intermittent turbulence model for the dynamics of the magnetotail [*Chang*, 1998]. The theory is based on the overlapping resonances of plasma fluctuations. It provides a physical picture of sporadic and localized merging of coherent magnetic structures of varied sizes. Such a picture seems to depict the observational properties of "bursty bulk flows" (sporadic localized reconnections) in the magnetotail [*Angelopoulos et al.*, 1996; *Lui*, 1998]. In this picture, the onset of substorm is due to a global nonclassical nonlinear instability and the dynamics of the magnetotail during the evolution of the substorm is characterized by the phenomenon of forced or self-organized criticality [*Chang*, 1998].

The consequence of this is the prediction of multifractal characteristics of the fluctuation spectra [*Hosino et al.*, 1994; *Milovanov et al.*, 1996; *Zelenyi et al.*, 1998; *Chang*, 1992; *Chang*, 1998; and references contained therein] and the dynamics of the magnetotail behaves essentially as a low dimensional system. This conclusion seems to agree with the results of some of the recent nonlinear dynamics calculations [*Baker et al.*, 1990; *Klimas et al.*, 1991, 1992, 1998; *Baker*, 1998].

If we accept this new paradigm of magnetotail dynamics, particularly during the periods of substorm evolution, it immediately indicates several directions of observational, numerical and laboratory investigations for the 21st millennium.

6.1. Observations

In the area of observations, it is obvious that more information in the direction of the fluctuation spectra will be needed. With the limitation of single spacecraft observations, the spectra that can be obtained based on present day observational capabilities will necessarily be restricted within the time domain. To convert these to the **k** spectra, some assumptions will have to be made. In the MHD domain, this is somewhat straightforward since the wave speed is essentially known. For the kinetic region, however, some information with regard to the wave modes must be available. In the future, when sophisticated coordinated multi-spacecraft observations are available, it might be useful to measure the multipoint correlation spectra as well.

It will also be useful if more statistically averaged information is obtained through observations. Since the turbulence is anisotropic and inhomogeneous, directional as well as spatial variations are needed as inputs in the development of specific theoretical calculations. After all, we still need to determine what is (are) exactly the global instability (instabilities) that is (are) responsible for the onset of substorms. There may be several different types of instabilities that can lead to the onset of substorms. There may also be several different classes of substorms, depending on the input of the global parameters; thereby leading to different characteristics of the fluctuation spectra.

6.2. Numerical simulations

Recent advances in global simulations have given some insights to the nature and characteristics of the global instability (instabilities) that are associated with the onset and evolution of substorms. However, since the global simulations generally depend on ad hoc assumptions of anomalous resistivity or numerically generated dissipation, these numerical results cannot provide any hint to the nature of the true connection between the localized (and at least partially kinetic) dissipative processes and the apparent dissipation that are required in most of the global simulation calculations. Recent numerical simulations of reconnection processes have made numerous advances in the understanding of localized reconnections. These results are particularly useful in the interpretation of the kinetic portion of the fluctuation spectra. However, such information alone will not be sufficient to bridge the gap of the global processes and the localized dissipations. An entirely different class of numerical simulations must be performed. The simulations must address the "large" magnetic Reynolds number problem, and the resulting turbulence must be anisotropic, inhomogeneous, and intermittent such that they are capable of resolving the generation, mixing, and merging of coherent magnetic structures as well as the interaction of these effects with macroscopic and microscopic fluctuations (including particle acceleration and diffusion) during substorms.

6.3. Laboratory simulations

There have been interesting laboratory simulations on magnetic reconnections. For example, there is the admirable work of *Yamada et al.* [1990] on the merging of MHD flux structures, and the equally fine observations on the whistler modes generated during electron MHD reconnection processes by *Stenzel et al.* [1996]. *Gekelman* and his collaborators [1997] have been making very interesting and accurate studies of the dynamics and merging of kinetic Alfvén resonance cones. It will be instructive (particularly to the theorists) when the work of *Gekelman et al.* and *Stenzel* are extended to the nonlinear regime of overlapping kinetic Alfvén and whistler resonances. Ultimately it will be useful in developing larger plasma chambers so that bonafide MHD intermittent turbulence may be conducted.

7. Addendum

In an interesting recent paper, *Chapman et al.* [1998] presented the simulation results of a simple avalanche model, that displayed many of the characteristic features (such as self-organized criticality and global instability, etc.) of magnetospheric activity that was advocated in this treatise.

Acknowledgments I am indebted to V. Angelopoulos, D. Baker, J. Büchner, S. Chapman, W. Gekelman, M. Hosino, J. Kan, C. Kennel, L. Kepko, M. Kivelson, A. Klimas, A. T. Y. Lui, J. Nicoll, H. Petschek, S. Sharma, R. Stenzel, D. Tetreault, D. Vassiliadis, D. Vvedensky, N. Watkins, C. C. Wu, and L. Zelenyi for useful discussions. A number of the conceptual ideas discussed in this paper is echoed in a recent book authored by *C. Kennel* [1995]. This research was partially supported by AFOSR, NSF, NASA and AFRL. The author wishes to thank B. Hultqvist and J. Geiss for their kind hospitality during his stay at the International Space Science Institute.

References

Angelopoulos, V., et al., *J. Geophys. Res.*, **101**, 4967, 1996.

Baker, D., et al., *Geophys. Res. Lett.*, **17**, 41, 1990.

Baker, D. N., in *Proc. 4th Intern. Conf. on Substorms*, edited by S. Kokubun and Y. Kamide, p. 231, (Terra Scientific Publishing Company, Tokyo, and Kluwer Academic Publishers, Dordrecht) 1998.

Büchner, J., in *Proc. 4th Intern. Conf. on Substorms*, edited by S. Kokubun and Y. Kamide, p. 461. (Terra Scientific Publishing Company, Tokyo, and Kluwer Academic Publishers, Dordrecht) 1998. See also, *Physics of Space Plasmas*, **15**. 383, 1998. (This volume).

Chang, T., *IEEE Trans. on Plasma Science*, **20**, 691, 1992.

Chang, T., in *Geospace Mass and Energy Flow*, edited by J. L. Horwitz, D. L. Gallagher, and W. K. Peterson, AGU Monograph Number 104, p. 193, (American Geophysical Union, Washington, D.C.) 1998.

Chang, T., D. D. Vvedensky, and J. F. Nicoll, *Physics Reports*, **217**, 279, 1992.

Chapman et al., *Geophys. Res. Lett.*, **25**, 2397, 1998.

Drake, J., Focus talk at the *IPELS Workshop on interrelationship between experiments in laboratory and space plasmas* held in Maui, Hawaii in June 1997. (See web site: http://ipels.physics.ucla.edu/ipels).

Galeev, A. A., M. M. Kuznetsova, and L. M. Zeleny, *Space Science Reviews*, **44**, 1, 1986.

Gekelman, W., S. Vincena, and D. Leneman, *Plasma Phys. and Contr. Fusion*, **39**, 1997.

Grassberger, P., and I. Procaccia, *Physica*, **9D**, 189, 1983.

Hosino, M., et al., *Geophys. Res. Lett.*, **21**, 2935, 1994.

Kennel, C., *Convection and Substorms: Paradigms of Magnetospheric Phenomenology.* Oxford University Press, Oxford, England, 1995.

Kivelson, M., and L. Kepko, private communication.

Klimas, A. J., et al., *Geophys. Res. Lett.*, **18**, 1635, 1991.

Klimas, A. J., et al., *J. Geophys. Res.*, **97**, 12253, 1992.

Klimas, A. J., et al., in *Proc. 4th Intern. Conf. on Substorms*, edited by S. Kokubun and Y. Kamide, p. 669, (Terra Scientific Publishing Company, Tokyo, and Kluwer Academic Publishers, Dordrecht) 1998.

Lui, A. T. Y., *J. Geophys. Res.*, **101**, 4899, 1996.

Lui, A. T. Y., *Physics of Space Plasmas*, **15**, 233, 1998. (This volume).

Milovanov, A., L. Zelenyi, and G. Zimbardo, *J. Geophys. Res.*, **101**, 19903, 1996.

Shan, L. H., C. K. Goertz, and R. A. Smith, *Geophys. Res. Lett.*, **18**, 1647, 1991.

Sharma, A. S., D. Vassiliadis, and K. Papadopoulos, *Geophys. Res. Lett.*, **20**, 335, 1993.

Stenzel, R., J. M. Urrutia, and C. L. Rousculp, *Physics of Space Plasmas*, **14**, 491, 1996.

Taylor, J. B., *Phys. Rev. Lett.*, **33**, 1139, 1974.

Tetreault, D., *J. Geophys. Res.*, **97**, 8531, 1992.

Vassiliadis, D. V., et al., *Geophys. Res. Lett.*, **17**, 1841, 1990.

Yamada, M., et al., *Phys. Rev. Lett.*, **65**, 721, 1990.

Zelenyi, L. M., A. V. Milovanov, and G. Zimbardo, in *The Earth's Magnetotail: New Perspectives*, AGU Monograph, Washington, D.C. American Geophysical Union, 1998.

New Results of the Theory of Non-Classical Polar Wind

Sunny W.Y. Tam, Fareed Yasseen[1] and Tom Chang

Center for Space Research, Massachusetts Institute of Technology, Cambridge, MA 02139, USA

Abstract. Recent *in situ* observations have revealed novel features in the polar wind. Measurements between 5000 and 9000 km altitude by the Akebono satellite indicate that both H^+ and O^+ ions have remarkably higher outflow velocities in the sunlit region than on the nightside. Electrons also display an asymmetric behavior: the dayside difference in energy spread, greater for upward-moving than downward-moving electrons, is absent on the nightside. Our previous calculations based on a self-consistent hybrid model [*Tam et al.*, 1995b] have demonstrated the significance of the anisotropic kinetic effects of photoelectrons in the dayside polar outflow. Results generated from the model agree with various qualitative features observed in the sunlit polar region by the Akebono satellite. Our recent work has extended the application of the model to the night-side polar outflow, in which photoelectrons are practically absent. By comparing the daytime and night-time results of our model, we demonstrate the anisotropic kinetic photoelectron effects on the polar outflow. In particular, the presence/absence of these suprathermal electron effects is responsible for the polar wind day-night asymmetries observed by the Akebono satellite.

1. Motivation

The existence of the polar wind, an outflow of plasma along the open magnetic field lines emanating from the polar region of the ionosphere, was first proposed by *Axford* [1968] and *Banks and Holzer* [1968]. These early studies recognized the ambipolar electric field as one of the mechanisms governing the plasma outflow. Because the polar cap, in general, is a relatively quiescent region, the ambipolar effect is a major contribution to the electric field in the "classical" polar wind, the steady-state, quasi-neutral, current-free outflow of plasma.

The ambipolar field itself exists self-consistently with the background plasma. It is therefore influenced by other mechanisms that need to be included in the dynamics of the particles. For example, the geomagnetic field, which decreases with altitude, gives rise to the mirror force that changes the particles' pitch angles. Coulomb interactions among all the species lead to energy exchange and pitch angle diffusion. These effects are essential to the dynamics of the particles, and therefore, can affect the polar wind electric field.

Recent observations have suggested that another effect, photoelectron populations generated in the sunlit ionosphere, can alter the polar wind significantly. Our study on the photoelectron-driven polar wind is motivated by these increasingly convincing experimental indications.

Early polar cap measurements obtained by the ISIS-1 satellite showed evidence of "anomalous" field-aligned photoelectron fluxes in both upward and downward directions, where the downgoing (return) fluxes were considerably smaller than the outgoing fluxes above a certain energy [*Winningham and Heikkila*, 1974]. Such non-thermal features were confirmed by the DE-1 and -2 satellites [*Winningham and Gurgiolo*, 1982]: outgoing field-aligned electron fluxes in the photoelectron energy range were observed by the HAPI (High Altitude Plasma Instrument) on DE-1 and the LAPI (Low Altitude Plasma Instrument) on DE-2; evidence of downstreaming electron fluxes was also found in the low-altitude distribution measured by the LAPI. These fluxes are considered anomalous because their existence cannot be related to the idea of thermal conductivity and temperature gradient in classical fluid theories. Similar to the ISIS-1 measurements, the return fluxes observed by DE-2 were comparable to the outgoing fluxes below some truncation energy, but considerably smaller above that. As suggested by *Winningham and Gurgiolo* [1982], the existence of such downstreaming fluxes may be due to reflection of electrons by the ambipolar electric field along the geomagnetic field line above the satellite. The truncation energy, obtained by comparing the outgoing and the return electron fluxes, would thus provide an estimate for the potential drop due to the electric field. These authors observed that this truncation energy ranged from 5 to 60 eV, and thus were able to deduce the magnitude of the potential drop above the altitude of the satellite ($\sim$ 500 km). Unfortunately, existing classical polar wind theories can only account for a much smaller potential drop [*Ganguli*, 1996, and references therein]. *Winningham and Gurgiolo* [1982] also pointed out that variation of the truncation energy was due to changes in the solar zenith angle at the production layer below the satellite. The solar zenith angle is related to the photoionization rate, which itself is related to the local ionospheric pho-

[1]Now at Climate Change Secretariat, Bonn, Germany

toelectron density [*Jasperse*, 1981]. These observations therefore imply a relationship between the local photoelectron density below the satellite and the potential drop along the field line above it, and are consistent with the idea that the photoelectrons may significantly affect the ambipolar electric field.

While the observations discussed above have implied that photoelectrons may contribute to the dynamics of the polar wind, more recent evidence indicates that the polar wind characteristics themselves are affected by the photoelectrons. *In situ* measurements by the Akebono satellite have revealed novel features in the polar wind: day-night asymmetries in the ion and electron features. The most dramatic are asymmetries in the ion outflow velocities [*Abe et al.*, 1993b]: satellite data between 5000 and 9000 km altitude have indicated remarkably higher outflow velocities for the major ion species, H^+ and O^+, in the sunlit region than on the nightside. For example, the H^+ velocity (u_h) was found to be about 12 km/s on the dayside, but only about 5 km/s on the nightside. Similarly, the O^+ velocity (u_o) in the sunlit region ($\sim$ 7 km/s) is about twice that in the midnight sector ($\sim$ 3 km/s). A day-night asymmetry was also observed in the electron behavior. Electrons were distinguished according to their velocities along the geomagnetic field line. On the dayside, it was found that the temperature of the upstreaming population is greater than that of the downstreaming population, *i.e.*, $T_{e,up} > T_{e,down}$, indicative of an upwardly directed heat flux [*Yau et al.*, 1995]. On the nightside, in contrast, no such up-down anisotropy was observed [*Abe et al.*, 1996].

Besides the day-night asymmetries, Akebono measurements between 5000 and 9000 km altitude have also revealed other sometimes unexpected ion transport properties in the polar region [*Abe et al.*, 1993b]. For example, O^+ was most often found to be dominant over H^+ as the major ion species, contrary to the traditional belief that very few O^+ ions are able to overcome the gravitational force and escape to such high altitudes due to their heavier mass. The measured outflow velocities for both the H^+ and O^+ ions in general increase monotonically with altitude, and the flows for both species are supersonic at high altitudes. In fact, the measured O^+ outflow velocities (see above) are much larger than the values expected by classical polar wind models [e.g. *Schunk and Watkins*, 1981, 1982; *Blelly and Schunk*, 1993]. All these ion outflow characteristics, particularly the enhanced ion outflow velocities, suggest a higher ambipolar electric field than that predicted by classical polar wind models [*Ganguli*, 1996, and references therein], and are consistent with the values of the field-aligned potential drop deduced by *Winningham and Gurgiolo* [1982] based on the DE-2 measurements.

Because of the marked day-night asymmetries observed in several characteristics of the polar wind, and the fact that photoelectrons exist primarily in the sunlit ionosphere, they are *the* natural candidate to account for the day-night asymmetries. Indeed, collisionless kinetic calculations by *Lemaire* [1972] showed that escaping photoelectrons may enhance the electric field and increase the ion outflow velocities in the polar wind. Photoelectrons, therefore, may provide a possible explanation for the observations of both sets of satellites: the magnitude of the ambipolar electric field deduced from the DE-2 measurements, and the day-night asymmetries and enhanced ion outflow velocities observed by the Akebono satellite. Because Coulomb collisions may also influence the dynamics of the photoelectrons, for example, by transferring their energy to other particle components in the polar wind, and thereby reducing the escaping photoelectron flux, collisional effects should also be taken into account in determining the impact of photoelectrons on the electric field. Our goal, therefore, is to address these observations by incorporating the complete photoelectron physics into a self-consistent, global description of the polar wind.

2. Photoelectrons, Energy Fluxes and Electric Field

The global kinetic collisional physics of suprathermal electrons in a steady-state space plasma outflow was first considered by *Scudder and Olbert* [1979] in their study of the solar wind halo electrons. These authors related the anomalous field-aligned electron heat fluxes observed in the solar wind to the non-local nature of the electron distributions, and demonstrated the formation of such non-thermal features using a simplified collisional operator. They also suggested that these suprathermal electrons, through their anomalous contribution to the energy flux, may significantly increase the ambipolar electric field along the magnetic field lines, thereby "driving" the solar wind [*Olbert*, 1982].

An analogous situation exists for the dayside, photoelectron-driven polar wind. It has been shown by *Yasseen et al.* [1989] that the polar wind photoelectrons can give rise to the non-thermal distributions observed by the DE satellites [*Winningham and Gurgiolo*, 1982]. The effect on the polar wind due to the energy fluxes associated with these photoelectrons has been examined by *Tam et al.* [1995a], who concluded that such anomalous electron energy fluxes may significantly increase the ambipolar electric field. Because photoelectrons exist primarily in the sunlit ionosphere, they enhances the dayside ambipolar electric field, thereby increasing the ion outflow velocities on the dayside. Photoelectrons, with their associated energy fluxes, can therefore provide not only a mechanism for the enhanced ion outflow velocities observed by the Akebono satellite [*Abe et al.*, 1993a, 1993b], but also the explanation for the observed day-night asymmetric ion and electron features in the polar wind [*Abe et al.*, 1993b, 1996; *Yau et al.*, 1995].

Energetic suprathermal electrons in the polar wind or in other ionospheric/magnetospheric settings have been considered by various authors. For example, kinetic collisional calculations by *Khazanov et al.* [1993] have examined the role of photoelectrons on plasma-

spheric refilling. Collisionless kinetic calculations by *Lemaire* [1972] have shown that escaping photoelectrons may increase the ion outflow velocities in the polar wind. Collisionless kinetic calculations by *Barakat and Schunk* [1984] and generalized semi-kinetic (GSK) calculations by *Ho et al.* [1992] have examined the impact of hot magnetospheric electrons, and concluded that such particles may also increase the ion outflow velocities.

We should add that other mechanisms besides suprathermal electron effects may also be proposed as alternative explanations for the enhanced ion velocities. Parallel ion acceleration driven by $\mathbf{E} \times \mathbf{B}$ convection was considered by *Cladis* [1986], and shown to significantly energize O^+ ions escaping to the polar magnetosphere. This force can also be seen as a centrifugal force in the convecting frame of reference, and was included in this form in the time-dependent, GSK model developed by *Horwitz et al.* [1994]. These mechanisms, including the suprathermal electron effects, have recently been reviewed by *Ganguli* [1996].

Recently, a self-consistent hybrid model has been developed by *Tam et al.* [1995b] to take into account the global kinetic collisional nature of the polar wind physics introduced by the photoelectrons. The details and advantages of the model have recently been discussed by *Tam et al.* [1998]. Our results in this paper are based on the model. The model represents two breakthroughs in polar wind theoretical modeling. One, it was the first to successfully incorporate the global kinetic collisional photoelectron effects into a self-consistent polar wind description. Two, due to its kinetic treatment of the ions, the model was the first to generate self-consistent global polar wind calculations whose solutions span continuously from a collisionless subsonic regime at low altitudes to a collisional supersonic regime at high altitudes.

The model is hybrid in that it consists of a kinetic and a fluid component. Photoelectrons (treated as test particles because of their low relative density) and both the H^+ and O^+ ions are described using a global kinetic collisional approach while thermal electron properties (density, drift velocity, and temperature) are determined from a simpler, fluid approach that also calculates the self-consistent ambipolar electric field. Because of its treatment of the thermal electrons, the model should be distinguished from traditional hybrid approaches where electrons are treated as a massless neutralizing fluid. The model is based on an iterative scheme combining the kinetic and fluid calculations, that should converge to physically meaningful solutions.

Let us specify some criteria that will enable us to define more precisely our study of the polar wind. First, we will consider the polar wind only at altitudes above 500 km (which corresponds roughly to the polar orbits of DE-2). At such altitudes, neutral densities are low enough to neglect the "chemical" reactions such as photoionization, recombination, *etc.* Second, the magnitude of the geomagnetic field is such that the gyration period and Larmor radius, for all particle species, are much smaller than any relevant time or length scales. We can therefore use the guiding center approximation. Third, the gradients of the geomagnetic field are such that only transport *along* the geomagnetic field line is important. The time-dependent distribution function $f(t, s, v_\parallel, v_\perp)$ for a given particle species is therefore governed by the following collisional gyrokinetic equation:

$$\left[\frac{\partial}{\partial t} + v_\parallel \frac{\partial}{\partial s} - \left(g - \frac{q}{m} E_\parallel\right) \frac{\partial}{\partial v_\parallel} - {v_\perp}^2 \frac{B'}{2B}\left(\frac{\partial}{\partial v_\parallel} - \frac{v_\parallel}{v_\perp}\frac{\partial}{\partial v_\perp}\right)\right] f = \frac{\delta f}{\delta t} = Cf, \quad (1)$$

where s is the distance along the magnetic field line B, q and m are the algebraic electric charge and mass of the species respectively, $E_\parallel$ is the field-aligned electric field, g is the gravitational acceleration, $B' \equiv dB/ds$, $\delta f/\delta t$ represents the rate of change of the distribution function due to collisions, and C is a collisional operator for Coulomb interaction, which is the dominant type of collision above 300 km altitude. Note that the operator C for a given particle species describes not only Coulomb collisions with other species, but also those among the same species itself. Equation (1) thus includes all the major forces a particle experiences as it travels along the geomagnetic field line: gravitational force, field-aligned electric force, mirror force, and forces that are due to Coulomb collisions, including those with the same species. The time-independent version of Eq. (1) is the governing equation in the kinetic component of our model.

3. Day-Night Asymmetries in the Polar Outflow

The main goal of this paper is to demonstrate the observed day-night asymmetry of the polar outflow based on our study of the anisotropic kinetic photoelectron effects. Application of the self-consistent hybrid model to the sunlit polar region has generated results [*Tam et al.*, 1998] that are qualitatively and quantitatively consistent with polar wind observations [*Abe et al.*, 1993b; *Yau et al.*, 1995]. In this study, we characterize the night-time polar wind conditions with the absence of photoelectrons. Thus, we generate a night-time polar outflow solution by using the same boundary conditions as those for the daytime, except without the presence of photoelectrons, *i.e.* $n_s = 0$.

The density profiles of all the species in the daytime polar wind solution is shown in Fig. 1. Note that the photoelectron density n_s is small compared with the thermal electron density n_e. Our test-particle approach for photoelectrons is therefore justified. The small photoelectron density, however, does not imply that these suprathermal particles are insignificant to the overall polar outflow dynamics. Because of the relation between the electron energy flux (or heat flux) and the ambipolar electric field [*Tam et al.*, 1995a], one

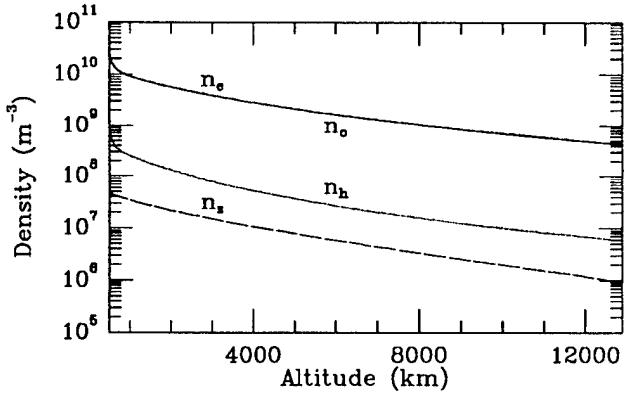

Figure 1. Density profiles for O^+ (n_o), H^+ (n_h), thermal electron (n_e), and photoelectron (n_s) in the dayside polar wind solution. Note that n_e and n_o are almost equal because of quasi-neutrality. Their lines virtually overlap in the plot.

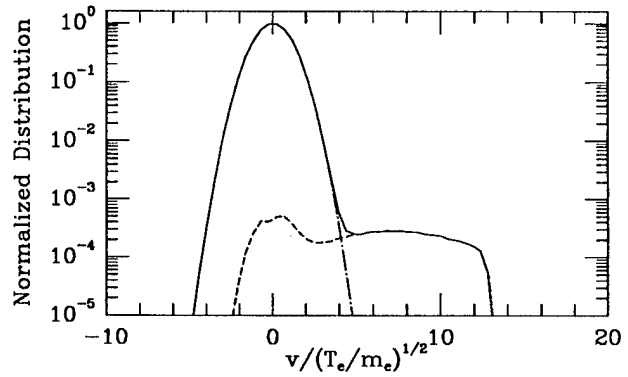

Figure 2. A typical normalized distributions for the combined electron population (thermal and photoelectrons) in the dayside polar wind (solid line). Dot-dashed line is for the thermal electron distribution; dashed line is for the photoelectrons. The distributions were calculated at 7500 km altitude. T_e is the temperature of the thermal electron population, and m_e is the electron mass.

has to examine the photoelectron heat flux contribution as well in order to determine whether the suprathermal population can significantly affect the outflow dynamics. Fig. 2 shows a typical normalized distribution for the combined electron population in our dayside solution. The contributions from the thermal and photoelectrons are also plotted in the figure. Note that the tail portion of the distribution is dominated by the photoelectron population. Such a distribution suggests that the majority of the electron heat flux is carried by the photoelectrons. By comparing the heat flux contribution due to the thermal electron with that carried by the photoelectrons, we find that the heat fluxes carried by the two electron components are in opposite directions: downward for the thermal but upward for the suprathermal, as shown in the top panel of Fig. 3. We also find that the photoelectron heat flux is much larger in magnitude than its thermal counterpart, as shown in

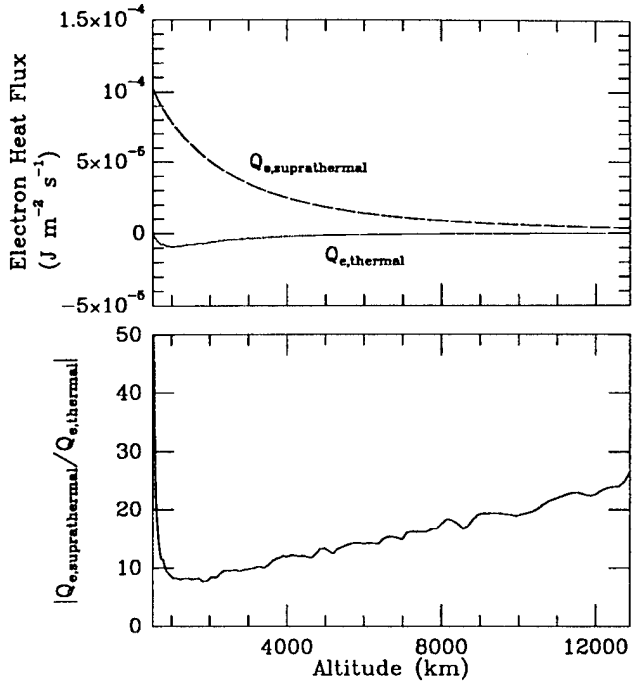

Figure 3. Top panel: heat fluxes carried by the thermal electrons ($Q_{e,thermal}$) and photoelectrons ($Q_{e,suprathermal}$) in the dayside polar wind solution. Note that the heat flux contribution by the thermal electrons is in the downward direction (negative sign) while that by the photoelectrons is upwardly directed (positive sign). Bottom panel: the ratio of the magnitudes of the two heat fluxes.

the bottom panel of Fig. 3. The two heat flux components combine to give the total electron heat flux whose direction is dictated by the photoelectron contribution, *i.e.* upward. The upwardly directed total electron heat flux is consistent with the data from *Yau et al.* [1995] and the results by *Tam et al.* [1995a, 1995b].

Due to the upwardly directed heat flux associated with the kinetic nature of photoelectrons, we expect the self-consistent ambipolar electric field to be larger in the dayside polar wind. That would give rise to a larger potential difference on the dayside, as compared with the nightside where photoelectrons are absent. Fig. 4 shows the self-consistent electric potential profiles for both polar wind solutions. The potential drop in the dayside solution is about 5 V, which is considerably larger than that on the nightside (about 2 V), and is comparable to value deduced from observations [*Winningham and Gurgiolo*, 1982].

The magnitude of the self-consistent ambipolar electric field has a significant impact on the ion outflow velocities. The O^+ and H^+ velocities in our two polar wind solutions are shown in Fig. 5. It is clear that both ion species have considerably smaller outflow velocities in the nightside results, in agreement with the observed day-night asymmetry in ion velocities [*Abe et al.*, 1993b].

The absence of photoelectrons in our nightside cal-

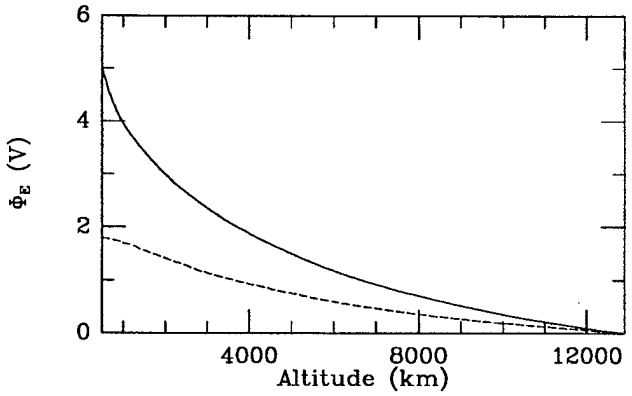

Figure 4. Self-consistent ambipolar electric potential profiles in the dayside (solid) and nightside (dashed) polar wind solutions.

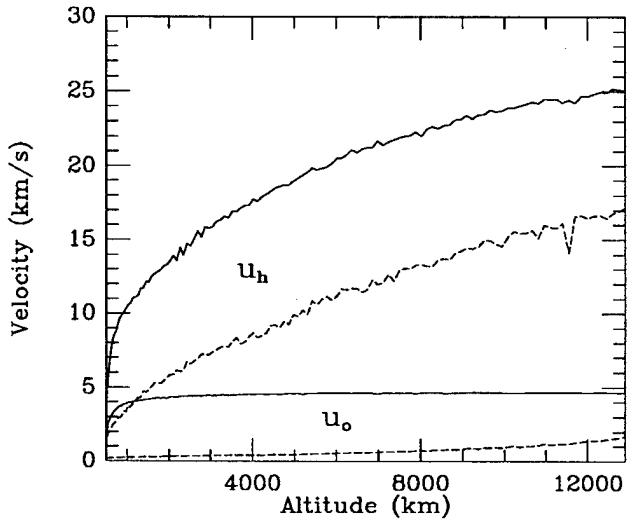

Figure 5. Profiles of ion outflow velocities in the dayside (solid) and nightside (dashed) polar wind solutions.

culations also leads to the absence of a noticeable electron anisotropy, in contrast to the dayside situation. The parallel temperatures for the upward- and downward-moving electron populations in both of our polar outflow solutions are shown in Fig. 6. The dayside solution reveals a temperature anisotropy between the upwardly and downwardly moving electrons, *i.e.* $T_{e,up} > T_{e,down}$ (the $\|$ subscript is omitted for simplicity). This anisotropy is entirely due to the photoelectrons. In the night-time solution, the temperatures for the two electron populations only differ by about 0.2% at the altitudes where the satellite measurements were made (900 – 1700 km) [*Abe et al.*, 1996]. The dayside and nightside electron temperatures together thus demonstrate the consistency between our photoelectron scenario and the day-night asymmetry observed by the Akebono satellite [*Yau et al.*, 1995; *Abe et al.*, 1996]. Because such a temperature anisotropy was observed in the dayside polar wind [*Yau et al.*, 1995] but seems absent on the nightside [*Abe et al.*, 1996], the role of

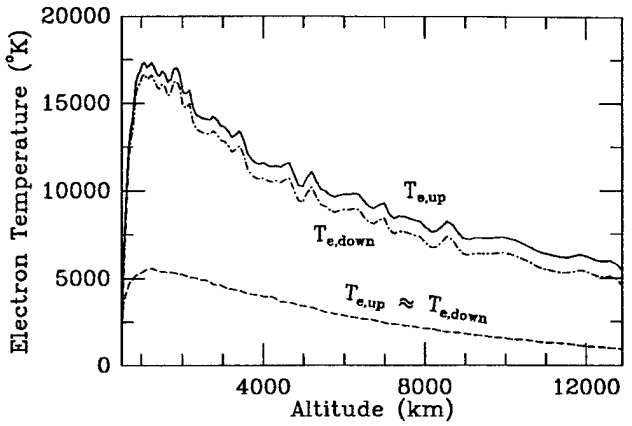

Figure 6. Parallel temperatures for upwardly and downwardly moving electrons, the $\|$ subscript has been omitted for simplicity. The dayside temperatures are represented by the solid and dot-dashed lines; the nightside temperatures, which are virtually equal for the two electron populations, are represented by the dashed line.

photoelectrons in our model is consistent with the observed polar wind scenario.

4. Conclusion

Our work on the polar wind is motivated by the increasing experimental evidence that photoelectrons may affect the dynamics of the polar wind. In particular, the day-night asymmetry in the ion and electron features suggests that photoelectrons may be *the* dominant effects in the polar outflow.

In order to study the impact of photoelectrons on the polar wind, we rely on a self-consistent hybrid model that provides a global kinetic collisional description for the polar wind photoelectrons. The model is hybrid in that it consists of a fluid part for the thermal electrons and a kinetic collisional part, and should be distinguished from other hybrid schemes where, for example, the electrons are treated as a massless neutralizing fluid. Specifically, in this model, photoelectrons (which are treated as test particles because of their low relative density), and all the ion species (H^+, O^+) are described by a global kinetic collisional approach, while thermal electron properties and the ambipolar electric field are determined by a fluid calculation.

In order to examine the anisotropic kinetic effects of photoelectrons as a source of the day-night asymmetry in the polar outflow, we have generated two polar wind solutions, one corresponding to the daytime outflow, and the other for the nightside. By comparing our dayside and nightside results, we have demonstrated the consistency between our photoelectron scenario and the observations. In particular, we have shown that the presence (absence) of photoelectrons on the dayside (nightside) may explain the observed day-night asymmetry in the polar outflow. For example, the anisotropy between the upward- and downward-moving

electrons, which is observed in the sunlit polar outflow but seems absent on the nightside, only appears in our dayside polar outflow results. We have also shown that the presence of photoelectrons leads to a considerably larger self-consistent ambipolar electric field, which corresponds to a larger electric potential difference along the magnetic field line. The magnitude of the ambipolar electric potential has a significant impact on the ion outflow velocities. Thus, both the H^+ and O^+ velocities in our results are remarkably higher on the dayside, in agreement with satellite measurements.

Acknowledgments The authors would like to thank J. D. Winningham, Andrew Yau, and Takumi Abe for many useful discussions with regard to the experimental data, John Retterer for participating with them in the initial stage of the investigation, and Supriya Ganguli for constant collaboration. This work is supported by NSF Grant ATM-9634599, AFOSR Grants F49620-93-1-0287 and F49620-96-1-0340, NASA Grant NAG5-2255, and AF Contract F19628-91-K-0043.

References

Abe, T., et al., *Geophys. Res. Lett.*, **20**, 2825, 1993a.

Abe, T., et al., *J. Geophys. Res.*, **98**, 11191, 1993b.

Abe, T., et al., in *Physics of Space Plasmas (1995)*, edited by T. Chang, and J. R. Jasperse, no. 14, p. 3, Cambridge, MA. MIT Center for Theoretical Geo/Cosmo Plasma Physics, 1996.

Axford, W. I., *J. Geophys. Res.*, **73**, 6855, 1968.

Banks, P. M., and T. E. Holzer, *J. Geophys. Res.*, **73**, 6846, 1968.

Barakat, A. R., and R. W. Schunk, *J. Geophys. Res.*, **89**, 9771, 1984.

Blelly, P. L., and R. W. Schunk, *Ann. Geophys.*, **11**, 443, 1993.

Cladis, J. B., *Geophys. Res. Lett.*, **13**, 893, 1986.

Ganguli, S. B., *Rev. Geophys.*, **34**, 311, 1996.

Ho, C. W., et al., *J. Geophys. Res.*, **97**, 8425, 1992.

Horwitz, J. L., et al., *J. Geophys. Res.*, **99**, 15051, 1994.

Jasperse, J. R., in *Physics of Space Plasmas*, edited by T. S. Chang, B. Coppi, and J. R. Jasperse, no. 4 in SPI Conference Proceedings and Reprint Series, p. 53, Cambridge, MA. Scientific Publishers, Inc., 1981.

Khazanov, G. V., et al., *Geophys. Res. Lett.*, **20**, 2821, 1993.

Lemaire, J., *Space Res.*, **12**, 1413, 1972.

Olbert, S., *NASA Conf. Publ.*, p. 149, 1982.

Schunk, R. W., and D. S. Watkins, *J. Geophys. Res.*, **86**, 91, 1981.

Schunk, R. W., and D. S. Watkins, *J. Geophys. Res.*, **87**, 171, 1982.

Scudder, J. D., and S. Olbert, *J. Geophys. Res.*, **84**, 2755, 1979.

Tam, S. W. Y., F. Yasseen, and T. Chang, *Ann. Geophys.*, **16**, 948, 1998.

Tam, S. W. Y., et al., in *Cross-Scale Coupling in Space Plasmas*, edited by J. L. Horwitz, N. Singh, and J. L. Burch, no. 93 in Geophysical Monograph, p. 133, Washington D.C. American Geophysical Union, 1995a.

Tam, S. W. Y., et al., *Geophys. Res. Lett.*, **22**, 2107, 1995b.

Winningham, J. D., and C. Gurgiolo, *Geophys. Res. Lett.*, **9**, 977, 1982.

Winningham, J. D., and W. J. Heikkila, *J. Geophys. Res.*, **79**, 949, 1974.

Yasseen, F., et al., *Geophys. Res. Lett.*, **16**, 1023, 1989.

Yau, A. W., et al., *J. Geophys. Res.*, **100**, 17451, 1995.

5. PUBLICATIONS.

Scientific Papers

1. Abe, T., B. Whalen, A.W. Yau, E. Sagawa, and S. Watanabe, Akebono observations of thermal ion outflow and electron temperature in the polar wind region, *Physics of Space Plasmas*, 13, 3, 1996.

2. André, M. and Tom Chang, Ion heating perpendicular to the magnetic field, *Physics of Space Plasmas*, 12, 35, 1993.

3. André, M., and A. Yau, Theories and observations of ion energization and outflow in the high latitude magnetosphere, *Space Sci. Rev.*, 80, 27, 1997.

4. André, M., P. Norqvist, A. Vaivads, L. Eliasson, O. Norberg, A. Eriksson and B. Holback, Transverse ion energization and wave emissions observed by the Freja Satellite, *Geophys. Res. Lett., 21, 1915, 1994*

5. André, M., P. Norqvist, L. Andersson, L. Eliasson, A.I. Eriksson, L. Blomberg, R.E. Erlandson, and J. Waldemark, Ion energization mechanisms at 1700 km in the auroral region, *J. Geophys. Res.*, 103, 4199, 1997.

6. André, M., Waves and wave-particle interactions on auroral field lines, *J. Atmos. Terr. Phys.*, 59, 1687, 1997.

7. Basu, B., J.R. Jasperse, J.M. Retterer, D.T. Decker, and Tom Chang., Theory and observations of high frequency electrostatic plasma instabilities in the lower ionosphere, *Physics of Space Plasmas*, 12, 147, 1993.

8. Chang, Tom, and M. André, Recent developments of ion acceleration in the auroral zone, in *Geospace and Energy Flow*, edited by J. Horwitz et al., AGU Monograph Number 104, p. 115 (American Geophysical Union, Washington, D.C.) 1998.

9. Chang, Tom, Multiscale intermittent turbulence in the magnetotail, in *Proc. 4th Intern. Conf. on Substorms,* ed. by S. Kokubun and Y. Kamide, p. 231 (Terra Scientific Publishing Company, Tokyo and Kluwer Academic Publishers, Dordrecht) 1998.

10. Chang, Tom, Self-organized criticality, multifractal spectra, and intermittent merging of coherent structures in the magnetotail, *Proc. 1998 Intern. Plasma Astrophysics and Space Physics Conference,* ed. Buechner et al., Kluwer Academic Publishers, Dordrecht, Netherlands, 1998.

11. Chang, Tom, and M. André, Ion heating by low frequency waves, in *Auroral Plasma Dynamics*, edited by R.L. Lysak, AGU Monograph No. 80, p.207 (American Geophysical Union, Washington, D.C., 1993.)

12. Chang, Tom, Sporadic localized reconnections and multiscale intermittent turbulence in the magnetotail, in *Geospace and Energy Flow*, edited by J. Horwitz et al., AGU Monograph Number 104, p. 193 (American Geophysical Union, Washington, D.C.) 1998.

13. Chang, Tom, Low-dimensional behavior and symmetry breaking of stochastic systems near criticality-Can these effects be observed in space and in the laboratory?, *IEEE Trans. on Plasma Science*, 29(6), 691, 1992.

14. Chang, Tom, Lower hybrid collapse, caviton turbulence, and charged particle energization in the topside auroral ionosphere and magnetosphere, *Physics of Fluids*, B5, 2646, 1993.

15. Chang, Tom, Path integral approach to stochastic systems near self-organized criticality, in Recent Trends in Physics, *Nonlinear Space Plasma Physics*, edited by R. Sagdeev et al., American Institute of Physics, NY, p. 252, 1993.

16. Chang, Tom, Path integrals, differential renormalization-group and stochastic systems in space near criticality, *Intern. J. Engr. Science*, 30(10), 1401 1992.

17. Cheng, C.Z., and J. R. Johnson, A kinetic-MHD model for studying low frequency multiscale phenomena, , *Physics of Space Plasmas*, 14, 127, 1996.

18. Dum, C.T., and K.-I. Nishikawa, Two-dimensional simulation studies of the electron beam-plasma instability, *Physics of Plasmas*, 1, 1821, 1994.

19. Dum, C.T., Lower hybrid wave-particle interaction and auroral acceleration, *Physics of Space Plasmas*, 13, 155, 1996.

20. Dum, C.T., Weak and strong turbulence theory, *Physics of Space Plasmas*, 13, 75, 1995.

21. Ernstmeyer, J., and Tom Chang, Lightning-induced heating in the mesosphere, *Geophys. Res. Lett.*, 25, 2389, 1998.

22. Ganguli, S.B., Tom Chang, F. Yasseen, and J.M. Retterer, Plasma transport Modeling using a combined kinetic and fluid approach, *Physics of Space Plasmas*, 12, 393 1993.

23. Jasperse, J.R., B. Basu, J.M. Retterer, D. Decker, and Tom Chang, High frequency electrostatic plasma instabilities and turbulence layers in the lower ionosphere, in *Space plasmas: coupling between small and medium scale processes*, edited by M. Ashour-Abdalla, Tom Chang, and P. Dusenbery, AGU Monograph No. 86, p.77 (American Geophysical Union, Washington, D.C., 1994.)

24. Johnson, J.R., and C.Z. Cheng, Global mirror modes in the magnetosheath, *Physics of Space Plasmas*, 13, 361, 1996.

25. Johnson, J.R., and T. Chang, Nonlinear vortex structures with diverging electric fields, *Physics of Space Plasmas*, 14, 769, 1996.

26. Johnson, J.R., and Tom Chang, Nonlinear vortex structures with diverging electric fields and their relation to the black aurora, *Geophys. Res. Lett.*, 22, 1481, 1995.

27. Johnson, J.R., Tom Chang and G.B. Crew, A study of mode conversion in an oxygen-hydrogen plasma, *Physics of Plasmas*, 2, 1274, 1995.

28. Retterer, J.M., Tom Chang and J.R. Jasperse, Transversely accelerated ions in the topside ionosphere, *J. Geophys. Res.*, 99, 13189, 1994.

29. Retterer, J.R., J.M., Tom Chang and J.R. Jasperse, Lower hybrid collapse and charged particle acceleration, in Recent Trends in Physics, *Nonlinear Space Plasma Physics*, edited by R. Sagdeev et al., American Institute of Physics, NY, p. 252, 1993.

30. Tam, S.W.Y., F. Yasseen and Tom Chang, Further development in theory/data closure of the photoelectron-driven polar wind and day-night transition of the outflow, *Annales of Geophysicae*, 16, 948, 1998.

31. Tam, S.W.Y., F. Yasseen, Tom Chang, S.B. Ganguli, and J.M. Retterer, Anisotropic kinetic effects of photoelectrons on polar wind transport, 1995, in *Cross-scale Coupling Processes in Space Plasmas*, edited by J. Horwitz et al., *AGU Monograph* Number 93, p. 133 (American Geophysical Union, Washington, D.C.) 1995.

32. Tam, Sunny W.Y. and Tom Chang, The limitation and applicability of Musher-Sturman equation to two-dimensional lower hybrid wave collapse, *Geophys. Res. Lett.*, 22, 1125, 1995.

33. Tam, Sunny W.Y., F. Yasseen, Tom Chang, and S. Ganguli, Self-Consistent Kinetic Photoelectron Effects on the Polar Wind, *Geophys. Res. Lett.*, 22 (August 1 issue), 1995.

34. Tam, W.Y., F. Yasseen, and T. Chang, Day-night asymmetry of polar outflow due to the kinetic effects of anisotropic photoelectrons, in *Geospace and Energy Flow*, edited by J. Horwitz et al., AGU Monograph Number 104, p. 97 (American Geophysical Union, Washington, D.C.) 1998.

35. Tam, W.Y., F. Yasseen, T. Chang and S. Ganguli, Photoelectron effects in the polar wind, *Physics of Space Plasmas*, 13, 619, 1996.

36. Tam, W.Y., F. Yasseen, T. Chang, and S. Ganguli, kinetic photoelectron effects on the polar wind, , *Physics of Space Plasmas*, 14, 619, 1996.

37. Tetreault, D., Turbulent relaxation of magnetic fields: 1. Coarse-grained dissipation and reconnection, *Physics of Fluids*, 97, 8531, 1992.

38. Tetreault, D., Turbulent relaxation of magnetic fields: 2. Self-organization and intermittency, *J. Geophys. Res.*, 97, 8541, 1992.

39. Yau, A., and M. André, Source processes in the high latitude ionosphere, *Space Sci. Rev.*, 80, 1, 1997.

40. Yau, A.W., T. Abe, Tom Chang, T. Mukai, K.I. Oyama, and B.A. Whalen, Akebono observations of electron temperature anisotropy in the polar wind, *J. Geophys. Res.*, 100, 17451, 1995.

Books

1. "*Space Plasmas: Coupling between Small and Medium Scale Processes,*" AGU Geographical Monograph No. 86, edited by M. Ashour-Abdalla, Tom Chang and P. Dusenbery, (American Geophysical Union, Washington, D.C., 1995*).*

2. *"Physics of Space Plasmas: Controversial Issues and New Frontier Research in Geoplasmas,"* Volume 12, edited by Tom Chang and J.R. Jasperse, (Scientific Publishers, Inc., *Cambridge, MA 1993).*

3. *"Physics of Space Plasmas: Chaos, Stochasticity, and Strong Turbulence,"* Volume 13, edited by Tom Chang and J.R. Jasperse, (Center for Theoretical Geo/Cosmo Plasma Physics, Cambridge, MA 1995).

4. "*Physics of Space Plasmas: Multiscale Phenomena in Space Plasmas,*" Volume 14, edited by Tom Chang and J.R. Jasperse, (Center for Theoretical Geo/Cosmo Plasma Physics, Cambridge, MA 1996).

5. "Chandrasekhar Memorial Volume," Special Issue of the *International Journal of Engineering Science*, Volume 36, Edited by T. Chang and A.C. Eringen, Pergamon Press, Netherlands, 1998.